Focused Beam Reflectance Measurement for Monitoring the Extent and Efficiency of Flocculation in Mineral Systems

Alexander Senaputra and Franca Jones
Dept. of Chemistry, Curtin University, Perth, WA 6845 Australia

Phillip D. Fawell and Peter G. Smith
CSIRO Process Science and Engineering, Waterford, WA 6152 Australia

DOI 10.1002/aic.14256
Published online October 24, 2013 in Wiley Online Library (wileyonlinelibrary.com)

Focused beam reflectance measurement (FBRM), where a scanning laser focused through a sapphire window measures real-time reflected chord distributions without solids dilution, is attractive for characterizing flocculation performance. An enhanced measurement principle in new FBRM instruments has implications for flocculation studies, demonstrated using hematite in synthetic Bayer liquor. Comparisons of previous (M500) and new (G400) instruments were complicated by the impact of their different physical dimensions upon flocculation hydrodynamics, but the G400 clearly measured larger chords. The original measurement principle based on a reflected intensity threshold counts large low-density aggregates as multiple chords; in contrast, the change to "edge detection" (very low threshold) is more likely to see a single chord, an advantage for studying mineral systems (aggregates often >500 μm). The G400 also captures bimodal character in unweighted chord distributions, producing distinct peaks for aggregates and fines after suboptimal flocculation; such peaks are rarely well resolved in older FBRM. © 2013 American Institute of Chemical Engineers
AIChE J, 60: 251–265, 2014
Keywords: flocculant, flocculation, aggregate size, focused beam reflectance measurement, fines capture

Introduction

Characterizing aggregate dimensions

Flocculation of fine particle slurries to form fast settling aggregates is a key aspect of solid–liquid separation in most hydrometallurgical flowsheets, which typically involve at least one stage of gravity thickening. Aggregate properties such as size and structure (density/porosity, shape) dictate the settling rate and extend through to the settled bed. Various reviews have examined the relationship between aggregate properties and slurry dewatering characteristics, including the methods used to monitor these properties.[1,2] Stokes' law and its subsequent refinements can be used to relate aggregate size and density to settling rate; the form used by Heath et al.[3] is shown below

$$U_h = \frac{\bar{d}_{agg}^2\, g(\rho_s-\rho_l)\left(\frac{\bar{d}_{agg}}{d_p}\right)^{D_f-3}}{18\mu}\left(1-\phi_s\left(\frac{\bar{d}_{agg}}{\bar{d}_p}\right)^{D_f-3}\right)^{4.65} \quad (1)$$

where U_h is the hindered settling rate (m s^{-1}), ρ_s and ρ_l are the solid and liquid densities, respectively (kg m^{-3}), ϕ_s is the solid volume fraction, g is the gravitational acceleration (m s^{-2}), d_{agg} and d_p are the aggregate and primary particle size, respectively (m), D_f is the fractal dimension and μ is the dynamic viscosity (N s m^{-2}).

The challenge in any particle aggregation study is to obtain reliable characterization under relevant conditions. Aggregates, whether formed by charge-based coagulation or polymer-bridging flocculation, exhibit fragile structures of low-effective density, and are highly sensitive to any handling or treatment applied postformation. For "real" systems in which the particles are mostly micron-sized and the aggregates have the potential to approach millimeters, reaction times will be measured in seconds, shear effects will be heightened, and settling also becomes a consideration.

Direct characterisation of aggregate structure (typically through D_f) is complex and often time-consuming. Image analysis techniques, sometimes combined with settling rate measurements of individual aggregates,[4,5] requires sampling and very high dilution that alters structures. In practice, it is often sufficient to indirectly infer relative aggregate structural behavior from the variation in flocculation response (aggregate size, settling rate) at different solids concentrations.

A summary of common methods available for monitoring particle/aggregate size is represented in Figure 1, together with their expected size ranges and solids loading that can be tolerated for direct measurement. It must be acknowledged that this last point is somewhat subjective, as the practical solids loadings will often vary with particle size. These methods are also distinguished by whether they can be applied *in situ* or *ex situ*, the latter implying slurry has to be

Correspondence concerning this article should be addressed to P. D. Fawell at phillip.fawell@csiro.au.

© 2013 American Institute of Chemical Engineers

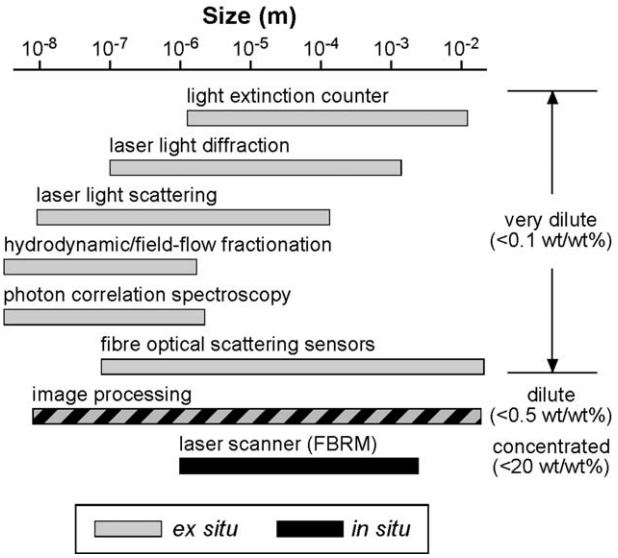

Figure 1. Optical methods for measuring geometry of particles in suspensions (adapted from Heffels et al.[6]).

sampled and possibly diluted for measurement. The essential criteria in the context of this discussion have to include applicability to flocculation at practical solids concentrations for mineral processing (as opposed to low solids water treatment).

The majority of techniques available for the sizing of particle systems fail when applied to polymer-flocculated aggregates in real-time studies. Although commercial particle sizing instruments that utilize laser diffraction or low angle light scattering have proven useful to characterize D_f for coagulated submicron latexes and other similar materials,[7] dilution is still necessary for the solids concentrations considered in most mineral systems and the measurements cells (even in a flow-through configuration) are likely to impose some shear to the fragile aggregates. The distributions that are obtained may also be of questionable value, given that they are unlikely to capture the often transitory real-time peaks in aggregate size, or may even represent artifacts of the sample handing (e.g., further growth on dilution). Optical/microscopic techniques cannot be applied during the aggregation process, and either require very high dilution or immobilization of the aggregates being studied. Turbidity fluctuations was not included in Figure 1 as it only offers a "flocculation index" as a relative indication of aggregation rather than a size, but has had some success for qualitative comparisons in water treatment applications.[8] However, this is again an instrument better suited to lower solids concentrations.

In the early 1990s, a new approach became available for monitoring particle and aggregate properties with the potential to be directly applied to suspensions across a wider concentration range. At times referred to as scanning laser microscopy, it is now better known by the more descriptive name of focused beam reflectance measurement (FBRM).

Principles of FBRM

In FBRM, a rotating lens provides a highly focused laser beam at the external surface of a sapphire window that scans in a circular path at a fixed velocity (Figure 2a). When the beam meets the suspended solids at the focal plane (Figure 2b), backscattered light is generated and the measured time lag between laser emission and reflection is multiplied by the velocity of the scanning laser to calculate a "chord" length. A chord for any geometric shape may be defined as the line segment whose endpoints both lie on the external surface of that shape. Thousands of chords can be measured during a single-measurement duration (as short as 2 s), generating a chord length distribution. Measurements occur in dilute or concentrated flowing slurry with no sampling or sample preparation necessary.

Figure 2b also demonstrates schematically how the chord distribution would appear for mono-dispersed spherical particles. The largest chord length is near the diameter ($2R$ in the figure), where there is a high probability of chords being measured, but shorter chord lengths will also be represented in the distribution.

Applications to flocculation

A number of groups have recognized that FBRM offers significant advantages for the study of flocculated systems, primarily through the ability to provide real-time *in situ* or in-stream information, avoiding the need for sampling and

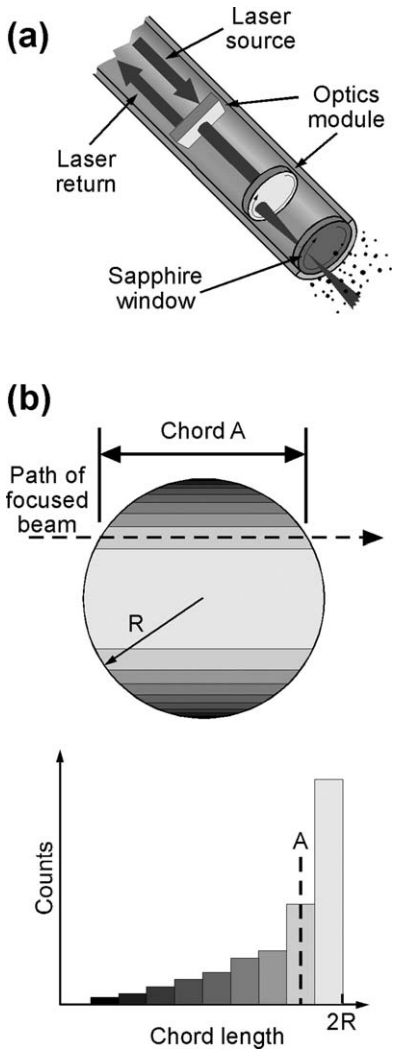

Figure 2. Schematic representations of (a) FBRM probe and particle sensing and (b) generation of a chord length distribution for mono-dispersed spherical particles.

dilution. Despite widespread use in a range of industries, studies of mineral systems have been rare and often lacking in detail. The US Bureau of Mines used an early FBRM system (Partec 100) for an *in situ* study of the shear aggregation of silica.[9,10] They observed that at higher mixing speeds large aggregates became unstable, resulting in a narrower distribution.

In a study of the centrifugal dewatering of polymer flocculated suspensions of manganese dioxide, Caron-Charles and Gozlan[11] used a Partec 100 to measure "size" distributions of the products formed. The dewatered cakes were suspended in clarified supernatant and mixed to allow the probe to be used. They considered the use of the Partec 100 to be suitable because it eliminated the need for high dilution, which may have modified the aggregate size.

Sengupta et al.[12] used FBRM to examine kaolin flocculation by a cationic polyacrylamide in a stirred glass beaker. They studied the effects of mixing speed and time, staged flocculant addition, pH, and solids concentration. Their main performance measure was a "relative size" term, being the ratio of the mean aggregate size over the primary particle size. More detailed studies were carried out by Peng and Williams.[13,14] They examined the flocculation of silica by cationic polyacrylamides in a stirred baffled vessel. By recording distributions every 16 s, they were able to extract information on the kinetics of both the flocculation and aggregate rupture processes. They were also able to show that, for this particular substrate, multistage addition of flocculant produced larger aggregates than a single dose.

Peng and Williams[15] completed a detailed investigation of aggregate rupture in pipe flow. Silica was flocculated in a 360-L stirred baffled tank by the addition of a cationic polyacrylamide. The tank was sealed and pressurized to control the flow rate through the pipe outlet. A Partec 100 probe was inserted at the base of the tank to allow aggregates to be characterized before entering the pipe. Aggregates were ruptured in a 0.8-m long pipe with a uniform internal diameter of 22 mm. A second probe was fitted at the end of this pipe, allowing the extent of aggregate rupture to be monitored as a function of the velocity gradient. From this, a quantitative assessment of aggregate strength could be obtained.

Flocculation of hematite in stirred beakers has been examined by FBRM and compared to classical settling and turbidity measurements.[16] The hindered settling rate and average chord length displayed similar trends with increasing dosage, while the total counts below 9.3 μm correlated with residual turbidity results. However, FBRM offered a real time continuous analysis of the reaction, compared to the batch settling rate and turbidity measurements.

A major concern with many FBRM flocculation studies has been the poor control of mixing. Batchwise mixing in stirred vessels is known to be inefficient, generating a wide range of shear rates with only particles close to the impellor experiencing high shear.[17] Residence times within the mixing zone are invariably higher than optimal, leading to aggregate rupture.

Blanco and coworkers used FBRM (now the M series, a significant upgrade on the early Partec instruments) in the study of flocculation in papermaking[18] and cements,[19,20] in both cases considering mixtures of mineral particles and fibers. They compared the extent of flocculation achieved with different flocculant products over time in stirred beakers and the capacity for reflocculation when the applied shear conditions are reduced. Such reflocculation is rare if ever observed in hydrometallurgical applications, for which the polymer-bridged aggregates are irreversibly ruptured on extended shear.[3]

Hecker et al.[21] inserted a similar FBRM probe below the settling tube of a Couette mixing device (the Shear Vessel) for a study of kaolin flocculation. They established some rough correlations between the mean square-weighted chord length and the hindered settling rates measured from flocculation at a fixed solids concentration with different flocculants. A scaled down version of this shear vessel was latter used with FBRM to examine flocculant make-up effects.[22]

The greatest control over flocculation conditions has come from using turbulent pipe flow, with FBRM detection and variation of pipe length after flocculant dosing allowing reaction times to be controlled to a fraction of a second.[23,24] Kinetic measurements of such real systems were only possible through FBRM use, leading to the development of a population balance model for polymer-bridging flocculation,[25] more advanced relationships between chord length statistics and settling rates[3] and new insights into the flocculation process.[26,27]

In their use of FBRM to monitor flocculation in papermaking, Blanco et al.[18] proposed a simple test that allowed semiquantification of aggregate strength, although this appears best used for direct product comparisons under selected conditions. Kirwan[28] extended this approach to bauxite residue flocculation to contrast the behavior of two flocculant systems. In a separate study of bauxite residue, Phillips[29] focused on the counts at the lower end of the chord length distribution to establish how different products impacted upon fines capture.

The potential for FBRM to provide number-sensitive information from unweighted chord length distributions and volume-sensitive information from application of length-square weightings is a significant advantage in flocculation studies, offering discrimination of flocculation efficiency and extent, respectively. That the results differ from classical particle sizing does cause some confusion. Thapa et al.[30] incorrectly described the counts from the unweighted chord length distributions as representing the number of particles; while the total counts can be number-sensitive, the relationship with number is certainly not linear and may be complex, especially when sizes (or shapes) are broad or changing. De Clercq et al.[31] were aware of this when submerging an FBRM at various locations within a full-scale municipal wastewater clarifier, but then only compared the unweighted chord length distributions, thus neglecting the impact of passage through the clarifier on the relative aggregate sizes.

Refinement of the FBRM approach

Despite the clear advantages of FBRM in many applications, there have also been limitations that cannot be ignored and, in some situations, may raise concerns as to the true relevance of the results. Greaves et al.[32] observed that for bimodal systems, large particles will often diminish the ability of FBRM to quantitatively measure small particles; certainly, this is the case for volume-weighted chord length distributions, although the unweighted distributions should still provide sensitivity to the fines. Vay et al.[33] determined that the FBRM response is influenced by the surface

characteristics of the tested materials (e.g., reflectivity, translucence), an issue when studying emulsions, but not really a concern for flocculation.

Heath et al.[34] noted the nonlinear response to increase in solids concentration, but potentially more significant was the tendency to oversize solids in the 1–10-μm range, a point also identified by others and can typically be attributed to the addition of the beam's width to the chord length.[33] Again, in flocculation studies, this does not impact upon the measurement of the volume weighted distributions used as an indication of the extent of flocculation. Such distributions are largely unaffected when flocculation is inefficient, whereas the unweighted distributions should show the impact of residual particles that are not captured within aggregates. This is certainly the case in many applications, but it is likely that the poor discrimination of sizes at the lower end of the distribution diminishes the sensitivity to such inefficiencies.

The G-series FBRM systems were developed to address some of these perceived problems. Of the improvements over the previous generation probes, the most significant were (a) higher resolution/greater accuracy in characterising fines particles and bimodal distributions, and (b) higher sensitivity in concentrated particle systems. Figure 3 is an attempt to represent in simple terms how such improvements have been achieved, using information from the manufacturer.[35] When backscattered intensity is measured as a reflection from the suspended solids, the intensity will vary, with surface roughness one factor that causes localized noise. Previous generation FBRM instruments applied a fixed intensity threshold above which the chord length will only be measured, however, when the localized noise from surface roughness is near the threshold limit (Figure 3a, Particle 3), some of the intensity will fall below this limit and register as the occurrence of several distinct chord lengths, when in reality there was only one particle. The new G-series instruments instead use enhanced edge detection to determine the measured chords, reducing the influence of surface roughness.

Another improvement in the new generation instruments is related to the consistency of the counts generated at higher solids loadings. As illustrated in Figure 3b, an increasingly dense population of particles obscures the laser intensity and in the older generation FBRM instruments, this resulted in a reduction in the measurement zone (represented by the hatching), which contributed to the nonlinear response of counts to solids concentration. For FBRM as achieved with the G-series instruments, the measurement zone is fixed (shading) and the nonlinearity of the solids response is greatly reduced.

The first image in Figure 3b shows that at low solids concentrations, the laser beam becomes quite diffuse at the extremes of the measurement zone, and for highly reflective particles, this could lead to chord length overestimation by older generation FBRM instruments if the fixed threshold was exceeded; for example, the measured chord length for Particle 5 in Figure 3a would be higher than the true value. In this case, edge detection with the G-series would lead to even greater overestimation, but combined with slope rejection, this chord is now rejected as out of focus. All these factors contribute to the potential for greater resolution and accuracy.

Objective of the present study

In many thickening applications, the feed properties are quite amenable to flocculation, that is, there are no colloidal

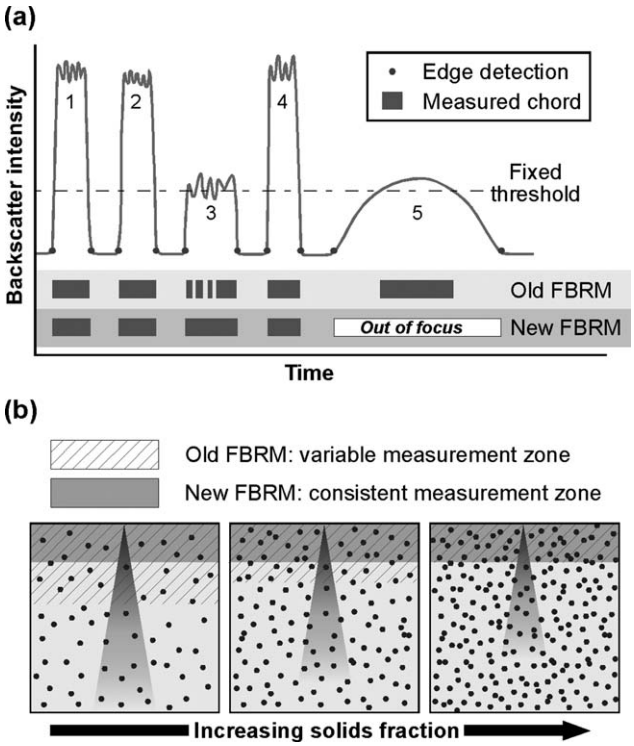

Figure 3. Schematic representations of (a) FBRM chord length detection methods and (b) the impact of solids concentration on FBRM measurement zones.

Adapted from Smith.[35]

solids and the surface chemistry favors flocculant adsorption. In such cases, the primary concern in characterizing the flocculation process is the extent of aggregation, through measuring the size achieved and relating this to settling rate or settling flux, for which the older generation FBRM instruments have proven valuable.

However, bridging flocculation with high molecular weight polymer flocculants becomes more problematic as the feed particle size becomes finer, with the aggregation process very much affected by the efficiency of flocculant distribution. High molecular weight flocculants become less effective when there is a high proportion of particles of micron size or smaller, with statistical analysis showing that the dosages required to achieve a good probability of chain adsorption become prohibitively high.[36] In addition, for some systems, the surface chemistry (either through mineralogy or pH) leads to a reduced fraction of the particle surface being available to flocculant adsorption, thereby impacting on subsequent aggregate growth. The extent of aggregation still remains important, but characterization of the efficiency of the process (i.e., the ability to capture fine particles) is also required, particularly, when then the nominally clarified liquors after thickening undergo downstream processing (e.g., precipitation, electrowinning, solvent extraction). It is in terms of monitoring flocculation efficiency in real time that it is believed that G-series FBRM may provide additional insights not achieved with the older generation instruments.

To test this premise, a synthetic system has been used to simulate bauxite residue flocculation. Alumina is extracted from bauxite in the Bayer process by digestion in caustic

liquors at elevated temperatures, producing insoluble residue phases suspended in high ionic strength solutions supersaturated in sodium aluminate. Such slurries must be thickened at ~100°C with high efficiency prior to the liquor undergoing precipitation. With the liquors being highly caustic and, therefore, not conducive to flocculant adsorption by conventional mechanisms, achieving the required level of flocculation is not a trivial process. Numerous studies have been conducted into how flocculant selection and flocculation conditions can impact upon the level of suspended solids within thickener overflows and the need for additional treatment prior to precipitation.[28,37] The synthetic system used here (with an iron oxide representing the residue phase) provides far greater reproducibility than plant or laboratory digested bauxite, as well as considerable scope to test the ability of G-series FBRM to reliably detect bimodal distributions after flocculation that may result from suboptimal flocculation conditions (whether that be from inadequate or excessive mixing).

Materials and Methods

The FBRM systems examined were M500 and G400, both obtained from Mettler-Toledo. The diameter of the probe tip immersed in the slurry was 25 mm for the old M500 version and 9.5 mm for the new G400 version. The M500 can be used with either "fine" or "coarse" electronics, the slower response of the latter enabling aggregates to be more reliably measured, but adding to the over-sizing of finer particles. Changing to the fine-electronics requires the physical swapping of an internal module, and therefore, the coarse-electronics was maintained throughout (in later D-series instruments, this change could be done through the flicking of a software switch). For the G-series, fine and coarse are now referred to as "primary" and "macro" chord selection models, and both are measured concurrently, with the ability to choose between the two depending on the application or aspect of greatest interest.

For both instruments, distributions were measured every 2 s and averaged over five measurements; the M500 provides distributions from 1 to 1000 μm, whereas the range for the G400 is extended to 4000 μm (these larger chord lengths could also be accessed by some of the D-series instruments). Particle and aggregate size distributions are usually presented as line graphs for ease of comparison, but in reality should be column graphs, with chord lengths divided into channels distributed in a logarithmic spacing. Such spacings are done in postprocessing and, therefore, do not affect data collection. The chords are integrated to give a "total counts" value (or counts up to a nominated chord length). A volume-weighting is achieved by applying a square-weighting to the chord length distribution.

$$n_{i,2} = n_i M_i^2 \tag{2}$$

where n_i and $n_{i,2}$ are the counts and square-weighted counts in a chord channel, respectively, and M_i is the chord length at the midpoint of the channel. The mean of this distribution is also derived

$$\text{Mean square-weighted chord length} = \frac{\Sigma_{i=1}^{k} n_i M_i^3}{\Sigma_{i=1}^{k} n_i M_i^2} \tag{3}$$

This work uses specific Bayer industry liquor properties terminology for describing liquor concentrations, of which A is aluminium in solution (expressed as g L^{-1} Al_2O_3), C (caustic) is sodium hydroxide plus sodium aluminate (expressed in terms of g L^{-1} Na_2CO_3), and S (soda) is C plus sodium carbonate (also expressed as g L^{-1} Na_2CO_3). The "testwork" liquor was made by adjusting a commercial sodium aluminate solution (Coogee Chemicals, WA) to target alumina and caustic concentrations (C = 230 g L^{-1}, A/C = 0.35, C/S = 0.99, liquor density (ρ) = 1200 kg m^{-3}) by using sodium hydroxide and deionized water.[38] Such concentrations were used throughout this study.

Iron oxides are typically a major component within residues from the digestion of lateritic bauxite feeds; Evans et al.[39] state that residues can be up to 60 wt/wt% Fe_2O_3. Hematite has often been used as a synthetic substrate to represent bauxite residue in studies of flocculant adsorption and flocculation performance,[40,41] the source varying in terms of the particle sizing required for the study. As this study sought to emphasize the impact of flocculation efficiency, a fine hematite powder from Sigma Aldrich (Iron (III) oxide, ≥99%) was used.

The flocculant products that can be applied in bauxite residue flocculation have been discussed elsewhere.[28,29,40] Although high-molecular weight acrylamide/acrylate copolymers are favored in most other tailings applications, high alkalinity leads to other mechanisms of flocculant adsorption and the use of distinct flocculant chemistries. The simplest of these are polyacrylate products, having little or no amide character; this was preferred over other flocculant chemistries as it is known to give relatively poor fines capture for residues having high fines contents. Alclar 665 (from BASF) was selected as a representative polyacrylate. Many comparable products are available and there is no implication that this was an optimized selection.

To prepare a 0.5 wt/wt% stock flocculant solution, Alclar 665 powder (1.0 g) in a glass jar was wetted with ethanol (1.5–2 g) before the required mass of deionized water was added and the jar sealed. This was placed on a shaking table and maintained in gentle motion for at least 24 h at room temperature to ensure full dissolution and close to equilibrium deagglomeration of polymer chains.[22] The stock was diluted to 0.0125 or 0.025 wt/wt% with a 20 g L^{-1} NaOH solution immediately prior to flocculation tests. The dosage of flocculant added into the system is expressed as grams of flocculant per tonne of hematite solids (g t^{-1}).

Slurries of different solids concentrations were prepared by adding a known amount of hematite to the testwork liquor, then preconditioned at a high mixing intensity (700 rpm, 70°C) for 15 min in a 2.5-L baffled stainless steel beaker (diameter 12.5 cm, height 25 cm) fitted with a 8.9-cm diameter A310 impeller. Testing indicated that the flocculation response for such slurries remained consistent for preconditioning times of up to 90 min, with some ageing effects apparent at longer times (i.e., a slow decline in the aggregate sizes attained). All testing was, therefore, completed within the 90 min period.

For the main flocculation tests, 150 mL of slurry was transferred to a water jacketed standard 500-mL tall-form glass beaker (internal diameter 7.0 cm, height 13 cm) and placed in the FBRM beaker stand (Mettler-Toledo), equipped a four-blade turbine impeller (each blade 2.1 × 0.8 cm, angled at 45°C, shaft 0.8 cm). The stand supports the FBRM probe in a vertical position near the inner wall of the beaker and above the impeller, such that slurry is directed toward the probe tip, ensuring good sample presentation.[42] Note that the M500 and G400 each have a dedicated beaker stand, and

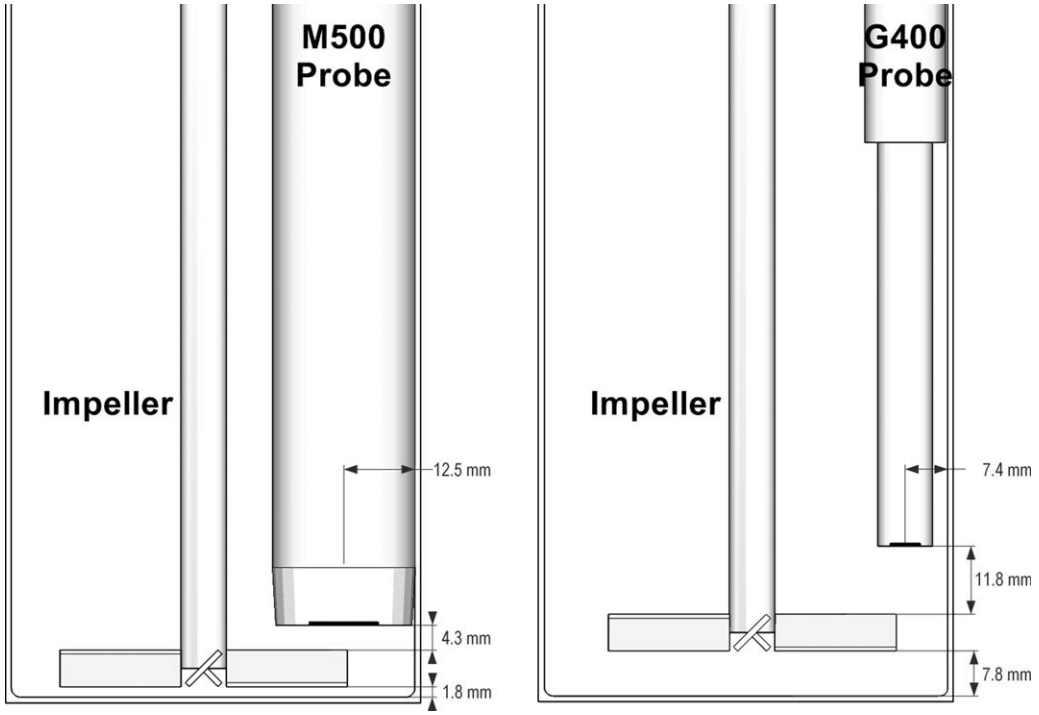

Figure 4. Beaker measurement geometry with M500 and G400 FBRM probes.

Sapphire window position on each probe shown by thick black line. Beaker, probe, and impeller dimensions are given in the text.

the different dimensions of the two probes leads to their positioning within the beaker being different (Figure 4). Unless otherwise stated, the stirring rate was fixed at 300 rpm throughout. The slurry was equilibrated at 70°C for 5 min before the required volume of dilute flocculant solution was injected.

To measure supernatant solid concentrations in selected slurries postflocculation in the G400 beaker stand, the same preparation and flocculation methods as described above were applied before agitation was stopped at a selected duration after flocculant addition. Settling was allowed to proceed for 60 s after this time, then supernatant (25 mL) was carefully removed with a syringe positioned ~1 cm below the liquor surface. This was vacuum filtered through a 0.45-μm membrane filter, washed by hot water (2 × 100 mL) to remove all salts and dried in an oven at 90°C, with the solids then determined gravimetrically.

Although examination of Figure 4 may suggest otherwise, neither beaker stand allowed both probes to be used simultaneously, as the probe bodies above the measurement heads are significantly wider. A larger scale geometry was, therefore, used for a limited number of flocculation tests monitored with both FBRM probes, as well as *in situ* imaging with a Particle Vision and Measurement probe (PVM, Mettler-Toledo). The PVM probe tip has identical dimensions to the M500 probe, with a number of strobing laser lights focused near the external surface of the sapphire window allowing images to be captured in stirred suspensions. The images as measured are 880 × 660 μm, with a resolution of 5 μm.

To accommodate the three probes, a water jacketted 5-L stainless steel baffled tank (diameter 16 cm, height 26.5 cm) was used in combination with an A310 impeller (diameter 8.6 cm). The probes were vertically positioned near the inner wall and in advance of the baffles, ~1–2 cm above the impeller.

Hematite slurry (2 wt/wt%, 2 L, $C = 230$ g L^{-1}, A/C = 0.35, and C/S = 0.99) held at 70°C was initially dispersed at high intensity mixing (700 rpm) for 15 min., with the stirring speed decreased to 300 ppm prior to addition of the flocculant (0.0125 wt/wt % Alclar 665). FBRM distributions were recorded every 2 s; PVM images were acquired at a rate of one per second with the manual control of the focal plane and contrast to get the best image quality.

Particle size distributions were also measured on selected samples by low angle laser light scattering with a Malvern Mastersizer 2000. Mie theory[43] is used to calculate the particle size from the scattering data through an iterative least square minimization matrix inversion process. No assumptions about the number of modes or breadth/narrowness of the distribution were made.

In contrast to FBRM tests, the Malvern measurements required high sample dilution and cannot be applied to slurries in the full-strength synthetic liquor. Sufficient sample was added to the analysis cell to obscure between 10 and 30% of the laser beam. To obtain a primary particle size distribution, hematite in water was treated with a dispersant (100 ppm sodium hexametaphosphate) and sonication applied prior to dilution and measurement. To obtain an indication of the likely extent of hematite coagulation in the synthetic liquor, sapphire windows were used with the Malvern instrument and hematite solids were physically dispersed (by stirring) in a 3 M NaCl solution at pH ~10; no dispersant was added. Surface area analyses were performed on washed and dried solid samples using a Micromeritics Tristar 3000 instrument.

Results and Discussion

Feed properties

The fully dispersed particle size distribution measured by laser light scattering (Malvern Mastersizer) is presented in

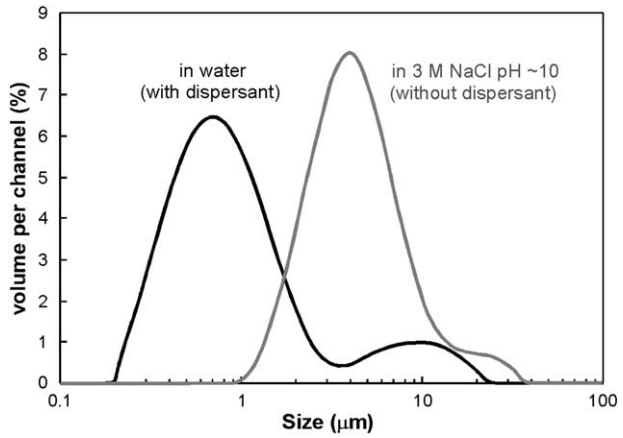

Figure 5. Particle size distribution for hematite (~0.05 wt/wt%) as measured by Malvern Mastersizer.

Figure 5, giving d_{10} 0.34 μm, d_{50} 0.76 μm, d_{90} 4.8 μm, and $d_{4/3}$ 1.80 μm. The measured specific surface area was 5.1 $m^2\ g^{-1}$.

It is immediately apparent from the fully dispersed hematite particle size distribution that the majority of the free particles (certainly on a number basis) are below the detection limit for FBRM. For a particle suspension with a significant submicron fraction, flocculation studies by FBRM are potentially complicated by the aggregation of effectively invisible submicron particles to larger sizes that can be detected would in fact see an apparent shift in the chord length distribution to lower sizes.

However, submicron solids are expected to be significantly coagulated within the highly ionic synthetic Bayer liquor, and the subsequent flocculation response will reflect the level of coagulation rather than the primary particle size, thereby substantially reducing the required flocculant dosages. The Malvern Mastersizer cannot be used with full strength Bayer liquors, and even with sapphire windows, the pH should ideally be kept at 10 or below. When suspended in 3 M NaCl at high pH prior to determining the particle size distribution, Figure 5 shows the hematite distribution to be significantly shifted to larger sizes relative to dispersion in water with the peak near 4 μm; significantly, almost nothing is seen below 1 μm.

Figure 6 shows the unweighted chord length distributions measured for hematite suspended in the testwork liquor using both the M500 and G400 FBRM probes under continuous stirring. The coarse-electronics and macro modes for each probe, respectively, represent the approach to chord length measurement that favors aggregate sizing (i.e., less likely to see them as distinct particles), but this reduces sensitivity to fines. They are observed here to give a similar peak near 20 μm, although the G400 distribution is broader, with some hint of a small shoulder at ~100 μm and more counts from 2 to 10 μm. The latter was expected, but at this stage, it cannot be said with any certainty if the former is a consequence of the refined measurement process. That no such shoulder exists in the primary distribution may suggest its presence in the macro distribution results from aggregation.

A significant shift in the distribution to smaller chord lengths was seen by changing the G400 processing from macro to primary, with the counts also elevated, although the peak was above 10 μm, still greater than that expected from the Malvern result in 3 M NaCl (Figure 5) acquired at a much lower solids concentration. Note that the counts below 2 μm remain lower that might be expected, which is not necessarily an indication of insensitivity to species at the lower end of the measurement range, but may instead reflect a greater impact of adding the beam width to these shorter chord lengths.[33]

Using the primary mode to examine aggregated solids may appear to be in conflict with normal expectations, and certainly, the macro mode would be used exclusively for examining the square-weighted (volume-weighted) chord length distributions and associated statistics when the extent of aggregation after flocculant addition (i.e., the aggregate size achieved) is the major goal. Access to the primary mode provides the ability to give some enhanced sensitivity to the low end of the distribution, and should at the very least, be considered when investigating fines formation or capture processes.

Flocculation: M500 vs. G400

Volume weighted FBRM results. A major attraction of using FBRM to monitor flocculation processes is the option of following a range of chord length statistics for a reacting system with measurement intervals as short as 2 s. Typical statistics used are shown below for flocculation with the G400 and M500 probes at two different dosages. Figure 7a presents the mean square-weighted chord length as a function of reaction time, used most commonly as the indication of aggregate dimensions. The corresponding results for the total unweighted counts over the full chord length range are given in Figure 7b as a guide to the efficiency of aggregation, although integrating the counts across a narrower chord length range (e.g., 1–10 μm) can be used in some instances to emphasize particular trends.

The reaction profiles for the mean square-weighted chord length data all show the expected response of a sharp rise upon flocculant addition, reaching a peak in aggregate size that is followed by a slower decline at longer reaction times. The corresponding profiles for the total counts display a minimum near the same reaction times as the peaks in size, beyond which the counts increase, consistent with the breakage or erosion of aggregates.

It is apparent from Figure 7 that the G400 results indicate a greater degree of aggregation. That the G400 total counts for the unflocculated solids were higher than the M500 value was an expected consequence of higher sensitivity, but fewer counts were observed by the former after flocculation (Figure

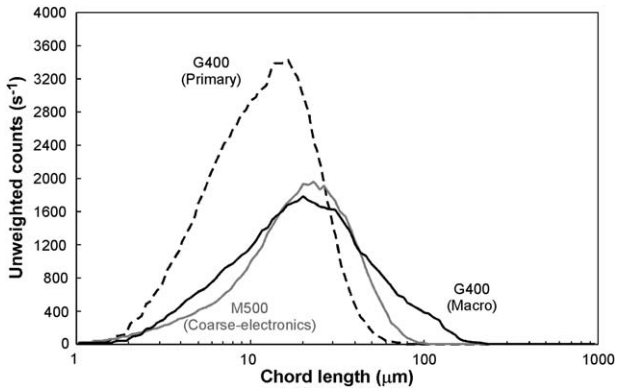

Figure 6. Unweighted FBRM chord length distribution for hematite (2 wt/wt%) within the testwork liquor, comparing the use of G400 and M500 instruments.

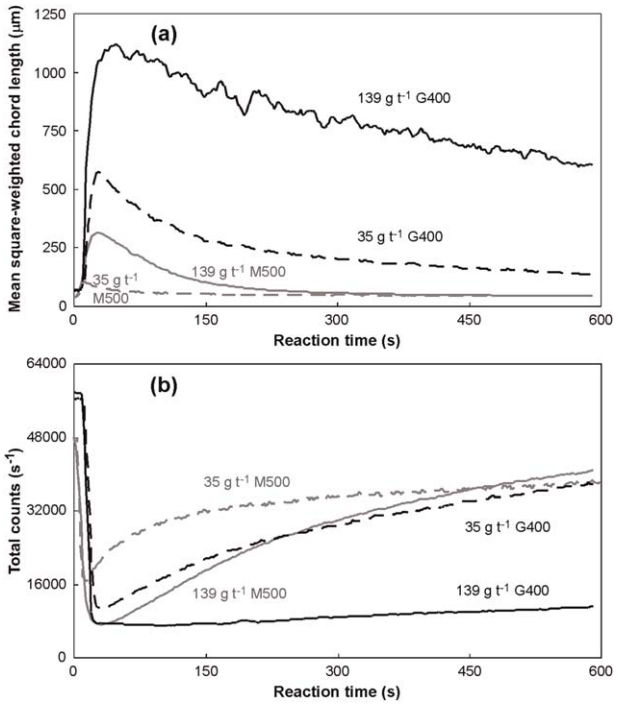

Figure 7. (a) Mean square-weighted chord length and (b) total counts for hematite flocculation (2 wt/wt%) at 300 rpm as a function of reaction time with G400 (macro) and M500 (coarse-electronics) instruments.

7b), while the mean square-weighted chord lengths were more than three times higher.

The interpretation of these results is complicated by the changed physical dimension of the G400 probe relative to the M500 (diameter 9.5 mm cf. 25 mm), combined with an altered positioning within the beaker stand arrangement (Figure 4). These factors inevitably lead to a change in the hydrodynamic conditions for flocculation, with the results obtained indicating a lower effective shear intensity experienced at the same rotation rate in the presence of the smaller probe, allowing larger aggregates to form and reducing the degree of aggregate rupture on extended mixing.

It is frequently assumed that mixing conditions within stirred vessels are determined by the impeller and its rotation rate; this may be the case for coagulation reactions for which aggregation is more likely in higher shear regions, but for polymer bridging flocculation processes it is expected that aggregates will grow in all vessel regions. As a consequence, the observed extent of aggregation after any reaction time, whether inferred from settling rate or aggregate size measurements, is an averaged response across products from all these zones.

To better understand the impact of the different hydrodynamics, a stainless steel sleeve was constructed for the G400 probe that increases its effective diameter to 25 mm, thereby allowing it to be inserted into the same beaker measurement configuration as the M500 probe (Figure 4). Figure 8 shows the square-weighted chord length distributions for both probes at selected reaction times at a fixed flocculant dosage of 139 g t^{-1}, confirming that the G400 probe is indeed observing much larger aggregate sizes. For comparison purposes, G400 results obtained in the absence of the sleeve are also shown, with the larger aggregate sizes able to be obtained at a much lower dosage.

Comparisons between two different geometries must, therefore, be viewed with caution, and will potentially create some issues for those who attempt to quantify aggregate breakage processes by FBRM within the beaker stand geometry.[18,28,44] It also highlights an important practical qualification that needs to be placed on all cylinder or stirred vessel tests, in that the flocculation performance measured is of relevance to the mixing conditions applied in that test, but not necessarily to those experienced within full-scale flocculation vessels (feedwells or feedpipes/launders). This concern was the primary motivation behind using turbulent pipe flow with FBRM detection for flocculation kinetics measurements, as the mean shear rate and reaction time can be controlled accurately, although requiring much larger sample volumes.[24,26,45]

Having considered the contribution from the measurement geometries, differences in the square-weighted chord length distributions in Figures 8 must be a consequence of the refined capabilities of the new generation probe. Most obvious is the impact of the expanded detection limit, which allows detection of chords up to 4000 μm and reliable measurements up to 2000 μm. Even with exercising caution and limiting the mean sizes measured to below 1500 μm, this still represents a significant extension beyond the capability of the M500 probe, for which mean sizes above 400 μm were rarely practical.

Although this extended range for the G400 probe may contribute to the differences seen in the 30 s distributions in Figure 8, it cannot be a factor in those for the longer reaction times. To better discern the true impact of the different processing approaches for the two probes, a limited number of experiments were conducted at a larger scale in which both FBRM probes and the PVM imaging probe were all used simultaneously in a baffled vessel (5 L total volume). The intention was that the images would provide some indication as to which FBRM probe was better capturing the

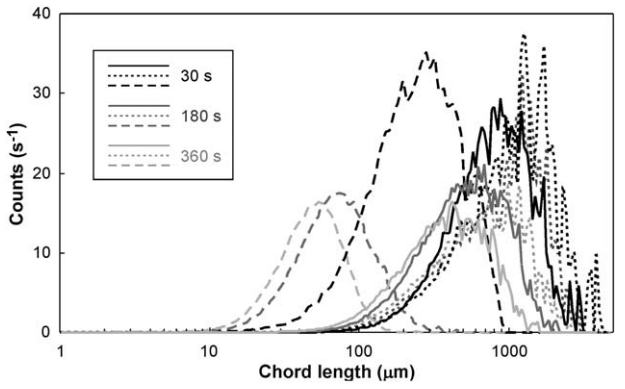

Figure 8. Square-weighted chord length distributions for different reaction times after flocculant addition to a hematite slurry (2 wt/wt%), comparing the use of M500 (coarse-electronics, long dashes) against G400 (macro mode, short dashes) at a dosage 139 g t^{-1}, with the latter in a stainless steel sleeve to match the hydrodynamic conditions of the former (Figure 4).

G400 results in the absence of the sleeve are also shown (dosage 69 g t^{-1}, solid lines).

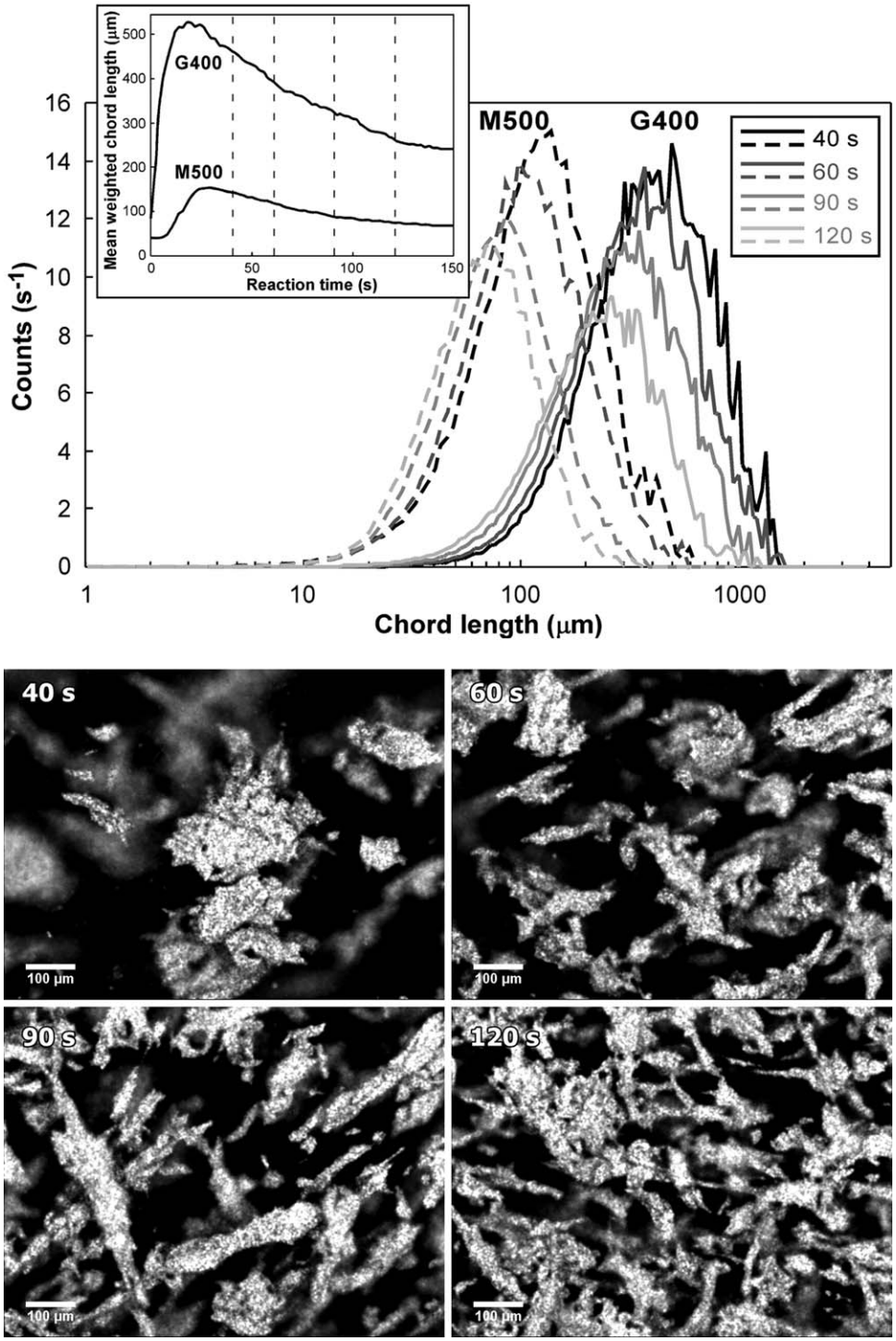

Figure 9. Effect of reaction time on square-weighted chord length distributions and the corresponding PVM images after flocculation of a hematite slurry (2 wt/wt%, dosage 139 g t^{-1}) in a 5-L baffled tank, comparing the use of G400 (macro, solid lines) and M500 (coarse-electronics, dashed lines) FBRM instruments.

actual aggregate properties. The PVM probe is more limited in the conditions that can be studied, with higher dilution preferred to minimize the overlap of aggregate boundaries; in this case 2 wt/wt% was the highest solids concentration that could be considered. Positioning of the probes to give comparable presentation was difficult and the vessel used represents yet another distinct hydrodynamic environment, but that was largely irrelevant to the purpose of achieving a degree of general validation. It should also be stressed that this larger vessel is far from ideal for detailed study of flocculation responses, given the broad shear rate distribution, and was only used to allow image acquisition with the FBRM results. Suitable presentation to the FBRM probes is obtained under milder mixing conditions with the smaller beaker geometry, making it better suited for comparison of flocculation efficiency.

The insert plot within Figure 9 shows the reaction profiles obtained from both FBRM probes and the four selected

reaction times for which the full distributions are given in the main plot. Again the aggregate sizes measured with the G400 probe are substantially larger than those from the older M500 across all reaction times, although the relative differential appears less than in the smaller scale tests. It can, therefore, be concluded that vessel hydrodynamics and the expanded measurement window for the G400 probe are not the only factors in the larger sizes observed in these flocculation studies.

The PVM images from the different reaction times were taken in a different physical location within the vessel from the FBRM data, and therefore, cannot be assumed to directly represent the chord length distributions from those times. However, the aggregates captured within each image do indicate that the M500 probe may be undersizing, particularly when examining the longer reaction times, at which the majority of visible aggregates extend well beyond 100 μm in one direction. Many of these aggregates are quite elongated, and chord length measurements will inevitably have a higher probability of producing shorter chords. This will undoubtedly influence the unweighted chord length distribution, but the very nature of the square-weighting process emphasizes the relative contribution of any larger chord lengths. That the square-weighted chord length distribution for the M500 probe sees a very low contribution from aggregates over 200 μm in size at a reaction time of 90 s is at odds with the image taken at that time.

It appears highly likely that the enhanced edge detection and removal of the fixed threshold for the G400 probe (as discussed in the Introduction) contribute to the reporting of larger chord lengths, and the square-weighting process serves to give them further emphasis. Considering the schematic in Figure 3a, aggregates may be considered as equivalent to "Particle 3," in that the old measurement principle may under size due to a single aggregate being reported as multiple smaller chord lengths. The use of the coarse-electronics with the M500 reduces this effect, but fractal aggregates become increasingly porous at larger sizes, reducing their potential to produce reflected chords across their full dimensions. If chord length measurement as performed with the G400 probe is increasing, this probability of seeing larger aggregates as a single body, then it may represent a major advantage, as these larger aggregates have a much greater practical significance to industrial flocculation processes.

Unweighted FBRM results. Figure 10 shows the unweighted chord length distributions obtained with both FBRM probes at different reaction times following flocculation in the 5-L baffled tank. As flocculation substantially reduces the total counts, these distributions can be almost an order of magnitude lower in their count scale in comparison to the corresponding unflocculated distributions (Figure 6), which can lead to an increased degree of noise. However, the flocculated distributions were still reproducible and highlight the distinctions between the two probes. Unweighted chord length distributions from the M500 system have often been used as an indication of flocculation efficiency, and can be seen here to display a clear increase in counts as the reaction time increased. However, results with the G400 probe provide greater sensitivity to the change in chord lengths as the aggregates are sheared. That larger aggregates are seen raises the prospect of better resolving the peaks from aggregates and fines, an aspect examined in more detail in the next section.

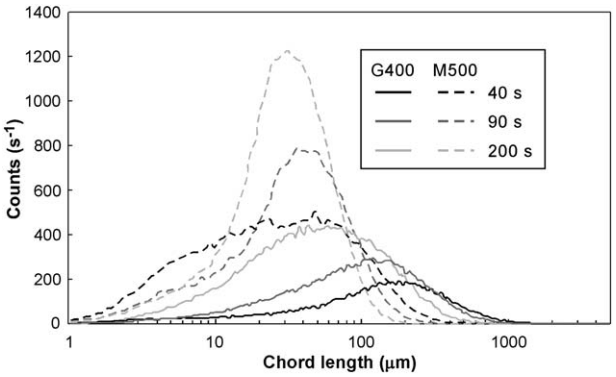

Figure 10. Unweighted chord length distributions at different reaction times after flocculation of a hematite slurry (2 wt/wt%, dosage 139 g t^{-1}) in a 5-L baffled tank, comparing the use of G400 (macro, solid lines) and M500 (coarse-electronics, dashed lines) FBRM instruments.

Any improved sensitivity to fines offers considerable scope for the optimization of flocculant selection and flocculation conditions for bauxite residue flocculation after digestion, for which effective fines capture is a primary concern, particularly if it reduces the need for filtration prior to product precipitation. The subsequent sections, therefore, only consider results for the G-series FBRM instrument. The small-scale beaker measurement geometry (with no sleeve on the G400 probe) was used, as this provided access to the mildest mixing conditions.

Effect of flocculant dosage

Understanding the flocculant dosage response is always a key aspect in any flocculation study, allowing the comparison of different flocculant products and ideally an indication of the effectiveness of the aggregation process. The dosage that produces the desired settling rate is not necessarily the same as that required for optimal fines capture.

Settling rate measurements from cylinder tests relate to the aggregate size and solids concentration, and are generally useful if the tests are done well. Supernatant clarity measurements are more problematic for tests done at the solids concentrations appropriate for thickening (they are of greater value in jar tests at very low starting solids concentrations). Settling mudlines within cylinders in the absence of any other flows can "drag-down" suspended solids, artificially enhancing the clarity result. Small-scale testing is considered to produce unreliable predictions of full-scale clarification performance, and yet this can often be a key priority in optimizing and controlling a process.

The effect of five different flocculant dosages (from 35 to 174 g t^{-1}) on the G400 FBRM flocculation response for a hematite slurry under constant mixing was examined, with the mean square-weighted chord length (Figure 11a) and total unweighted counts (Figure 11b) monitored as a function of time. As expected, higher dosages led to higher mean square-weighted chord lengths; while dosage increases beyond 104 g t^{-1} had a comparatively smaller impact on the peak size, on extended mixing it was apparent that the additional flocculant imparts a degree of strength to the aggregates, with significantly larger sizes maintained at a reaction time of 600 s.

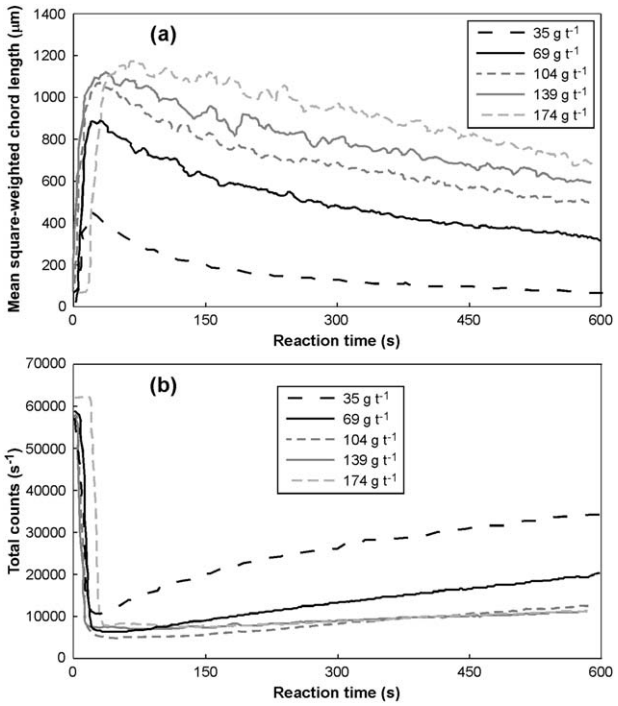

Figure 11. (a) Mean square-weighted chord length and (b) total counts as a function of reaction time for different flocculant dosages (G400 probe in macro mode, 2 wt/wt% hematite, 300 rpm).

Higher dosages also greatly reduced the total counts, with comparatively little change in the initial extent of this reduction beyond a dosage of 69 g t^{-1} (Figure 11b). Extended stirring had a greater detrimental effect at the lower dosages, again consistent with weaker aggregates leading to breakage and/or erosion processes.

Although the above interpretation of the total counts is useful, it only provides part of the picture, with the large reduction seen on flocculation actually masking detail that is best seen by considering the full unweighted chord length distributions after flocculation. Figure 12 shows these distributions at three dosages for three different reaction times. The macro mode for these distributions is shown; the primary mode gave additional counts and gave greater emphasis to the lower end of the distribution, but did not change the observed trends. For the lowest of these dosages (69 g t^{-1}, Figure 12a), the distribution after 30 s was clearly bimodal, with the lower peak at ~5 μm representing the contribution of fines and coagulated fines that were not yet flocculated, while flocculated aggregates made up the peak at ~300 μm. This was consistent with the short reaction time under fairly mild shear conditions giving suboptimal mixing, initially forming some very large aggregates but not efficiently capturing fines or microaggregates. Such peaks have never been so clearly resolved in unweighted distributions with the M500 probe.

Note that the large aggregates (>500 μm) that contribute most to the effective aggregate volume fraction will actually provide few counts to this distribution. Longer reaction times favor more efficient fines capture, almost eliminating the lower peak, but the fragile larger aggregates are readily ruptured, leading to the upper peak shifting to shorter chord lengths and higher intensity (i.e., a greater number of smaller aggregates).

The response was similar on increasing the applied dosage to 104 g t^{-1} (Figure 12b), although the upper peak was shifted to larger chord lengths and was of a lower intensity at all three reaction times shown. This is indicative of the higher dosage not only increasing aggregate size but imparting a degree of strength to the aggregates. However, analysis of data in this region is much better done through the weighted distributions that highlight the volumetric contribution and show distinct shifts in response to higher dosages; in contrast, the low counts at larger chord lengths in the unweighted distributions for higher dosages offer very little sensitivity to minor changes in conditions.

Figure 12b provides a hint of an increase in counts in the lower peak at a reaction time of 30 s, and this is clearly evident in Figure 12c for a dosage of 139 g t^{-1} for all three reaction times. Although this may seem counter to expectations for a high flocculant dosage that has produced larger aggregates, it is most likely a consequence of the mild mixing and the addition of a larger volume of flocculant contributing to localized overdosing, that is, a small fraction of the solids immediately contacted with the flocculant which is

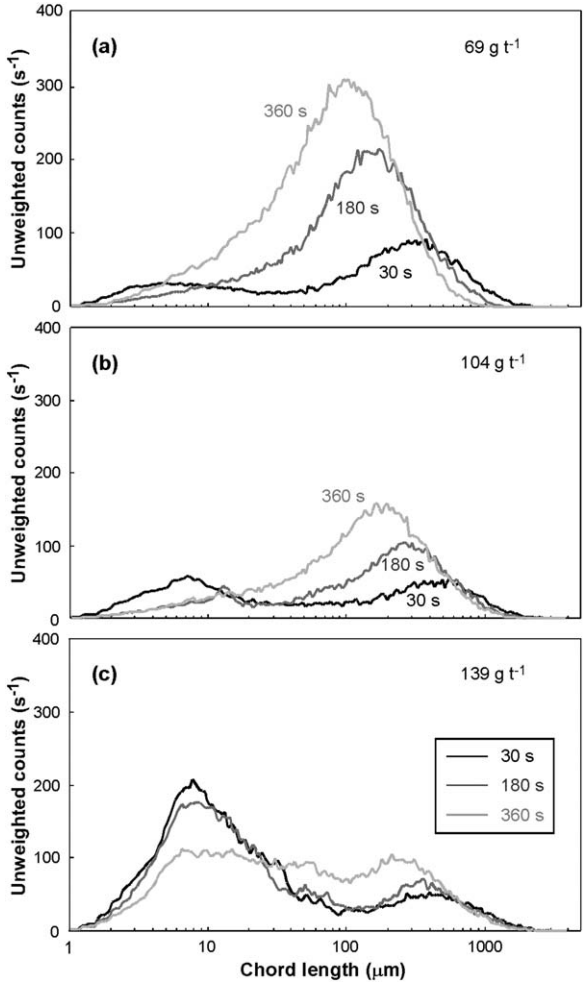

Figure 12. Unweighted chord length distributions at three different reaction times for flocculation at dosages of (a) 69, (b) 104, and (c) 139 g t^{-1} (G400 probe in macro mode, 2 wt/wt% hematite, 300 rpm).

Table 1. G400 FBRM Counts in Selected Chord length Ranges during Flocculation of Hematite (2 wt/wt%, 30 s reaction time) with Supernatant Solids Measured after 60 s of Settling

Dosage (g t^{-1})	Mixing (rpm)	Counts (s^{-1}): Primary Mode		Counts (s^{-1}): Macro Mode		Supernatant Solids (mg L^{-1})
		1–10 μm	1–20 μm	1–10 μm	1–20 μm	
35	300	992	1780	449	809	120
69	300	1080	1450	684	958	136
104	300	1570	2050	1020	1470	24
139	300	3330	4040	2180	2900	28
139	400	731	1020	445	651	84
139	500	2060	4410	751	1710	304
139	600	7410	16600	2060	4410	380

quickly adsorbed, leading to a high effective surface coverage. These particles or small aggregates are either thereby stabilized or at least have a reduced probability of being incorporated into larger aggregates, as is evident from the distributions after longer reaction times.

Table 1 compares the FBRM counts below 10 and 20 μm during flocculation (300 rpm, 30 s) at different dosages with the solids concentrations measured in supernatant samples taken 60 s after stirring was stopped. Interestingly, the supernatant solids results show a distinct step-change improvement in performance on increasing the dosage from 69 to 104 g t^{-1}, whereas the corresponding FBRM counts actually show significant increases. This highlights the nonequivalence of the two measures, with the supernatant solids measurement representing not only the 30 s reaction time under the applied mixing, but additional aggregation that can occur during the 60 s that follow, as well as any entrainment of fines by the settling aggregates. The latter in particular is expected to be enhanced by the formation of larger aggregates that then occupy a greater effective volume fraction.

Effect of applied mixing

As already discussed, estimating mean shear rates near impellers as a measure of the mixing intensity within stirred vessel used for batch flocculation is of little (if any) value, given that aggregation will also take place in the larger regions of lower shear.[17,23,27] That said, higher stirring rates will lead to more intense mixing and can provide useful qualitative comparisons.

Figure 13 shows the effect of increasing the applied mixing in the G400 beaker stand configuration on the observed unweighted chord length distribution. The volume-weighted distributions are not presented; they demonstrate the expected reduction in aggregate size and greater degree of breakage at longer reaction times, but in this case, it is the relative efficiency of flocculation that is of more interest. Increasing the stirring rate from 300 to 400 rpm leads to much more efficient fines capture, with only a slight contribution from the lower peak at the shorter reaction times but no evidence of it at 180 s. The better mixing achieved at 400 rpm ensures the flocculant is more effectively distributed even at this high dosage. In practical terms, it is often accepted that efficient fines capture comes at the cost of aggregate size and the corresponding settling rate.

The lower peak is absent in the unweighted chord length distributions at 500 rpm, but while fines capture may be good, the detrimental impact on aggregate size is readily apparent. At a reaction time of 180 s, the aggregate peak shifted to below 100 μm and was noticeably broadened, with an increase in counts below 20 μm. Flocculation was exceedingly poor at 600 rpm, and even though the peak position indicates aggregation, the majority of these aggregates are below 100 μm. At 180 s, the peak is shifted even lower and to higher counts, potentially masking any contribution from a fines peak.

The ability to clearly distinguish between conditions that do or do not favor fines capture represents possibly the most valuable enhancement from the G400 probe, providing far

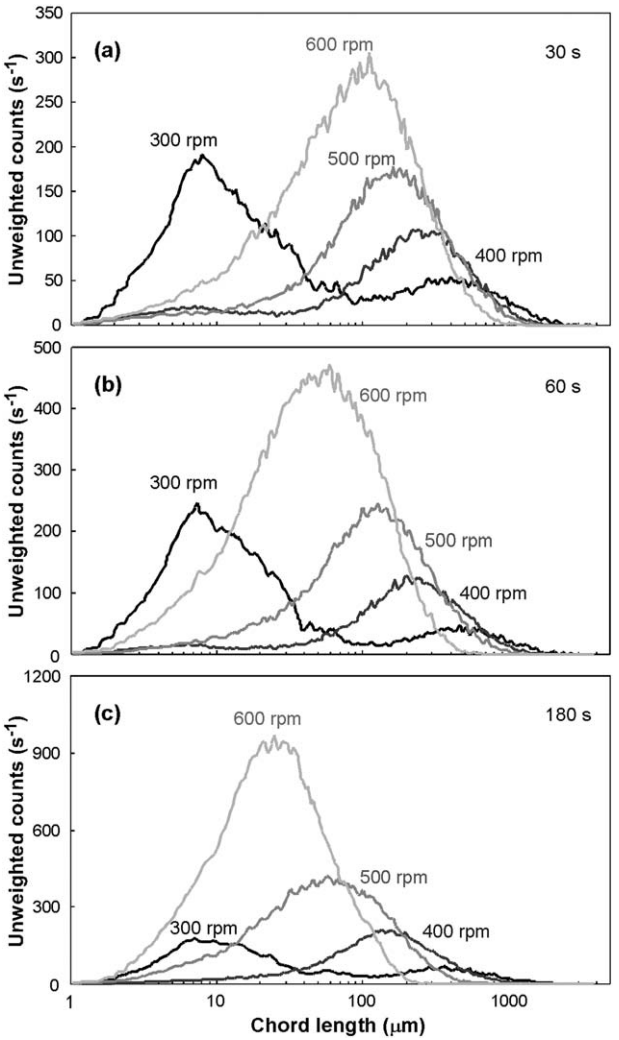

Figure 13. The effect of applied mixing on unweighted chord length distributions at three different reaction times for flocculation at a dosage of 139 g t^{-1} (G400 probe in macro mode, 2 wt/wt% hematite).

greater sensitivity than was ever seen with the earlier FBRM chord detection principles. In particular, this may offer major advantages in the screening of different flocculant products.

Supernatant solids concentrations were again determined following flocculation at each mixing intensity for 30 s and compared with the FBRM counts below 10 and 20 μm (Table 1). As was the case for the effect of dosage, the trends are different, although the effect of mixing did produce larger effects on both forms of measurement. Although FBRM suggested fines capture was best at 400 rpm, each increase in mixing intensity led to higher solids in the supernatant; the latter results are probably influenced by the reduced aggregate size. The enhanced counts for FBRM in primary as opposed to macro mode was evident in the results from different dosages, but the primary mode also proved much more sensitive to the effect of mixing. The substantial elevation in counts for primary vs. macro at 600 rpm also coincided with a significant shift to lower sizes. In this case the relative closeness in size between coagulated fines and small flocculated aggregates may prevent any resolution of their contributions in either distribution, but the variations between modes do at least indicate the presence of both.

Effect of solids concentration

The flocculation process is very much affected by the solids concentration, and in mineral systems, an optimum value is always observed; below this optimum, aggregation is often inefficient, while above it the aggregate size achieved will be limited by viscosity effects and the settling rates greatly reduced. One of the attractions of FBRM in the study of flocculation is its ability to be applied in real-time across a wide range of solids concentrations, and this has been discussed elsewhere.[24,26] The potential for application of the G400 probe to produce better information on aggregate sizes formed in high solids systems is of great interest, but is not relevant to the mineral system represented by the synthetic substrate/liquor examined here and will instead be the subject of a separate study. However, solids concentration effects were briefly considered in terms of monitoring flocculation efficiency with the G400 probe.

Figure 14 shows the effect of increasing the solids concentration on unweighted chord length distributions obtained with the G400 probe at two different reaction times. At 30 s, doubling the solids to 4 wt/wt% led to a slightly higher aggregate size after flocculation and an actual reduction in the fine counts below 20 μm, behavior maintained at the longer reaction time (120 s). This was clearly indicative of 4 wt/wt% being closer to the optimum concentration, although the lower concentration had served to provide greater sensitivity to variations in conditions (and as will described in a subsequent publication, flocculant selection).

The 30 s distribution on increasing the solids concentration to 6 wt/wt% suggests that the aggregate size was comparable and fines capture remained good. However, at 120 s, the aggregate peak was shifted to shorter chord lengths and higher counts, with more frequent aggregates collisions leading to an increased degree of breakage to midsized fragments.

At 8 wt/wt%, the aggregate size that can be formed becomes much more limited, and while some large chords near 1000 μm are measured at 30 s, the majority are centered around 200 μm. The inevitable long tail in the unweighted chord length distribution to the left of a peak means that the contribution of fines can no longer be readily inferred, although this may change at higher dosages. Increasing the reaction time to 120 s saw a very high degree of breakage, and the shift in the aggregate peak well to the left effectively merged it with the fines peak. This does not imply that the chord length information would necessarily lose its value for detecting flocculation inefficiency; comparison of the integrated counts below a selected chord length threshold under carefully controlled conditions would still provide an option for rapid screening.

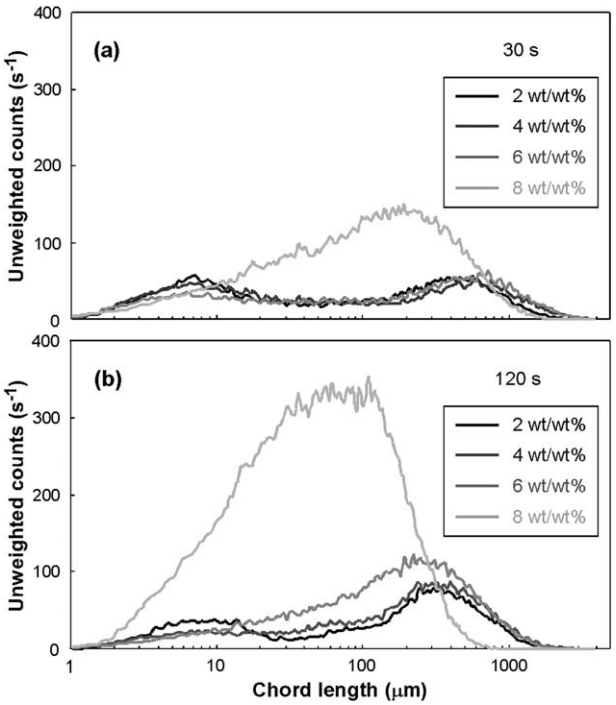

Figure 14. The effect of hematite solids concentration on unweighted chord length distributions at reaction times of (a) 30 s and (b) 120 s for flocculation at a dosage of 100 g t^{-1} (300 rpm, G400 in macro mode).

Practical Considerations

FBRM provides chord length information that is representative of the aggregation state under the conditions applied at the time of the measurement, and it must always be remembered that the conventional measures of flocculation performance are conducted under conditions that cannot be an exact match. Settling rates and supernatant clarities are acquired from batch tests in which there will inevitably be a delay after the applied mixing regime is completed. This delay represents a period of gentle (or tapered) mixing prior to the onset of mudline settling, with the potential for additional aggregate growth to occur and settling rates to be enhanced.[26] The same can be assumed for flocculated solids that are being discharged from a feedwell. Supernatant clarities from cylinder tests are measured after an even longer delay, and unflocculated or poorly flocculated fines detected by FBRM can be dragged down with large aggregates in mudline settling, leading to higher than expected clarities. Conversely, clarities in full-scale thickeners can be adversely affected by currents outside the feedwell entraining solids that would otherwise settle.

The mean square-weighted chord lengths reported from older generation FBRM for flocculated minerals are typically under 400 μm, and yet the naked eye can see much larger aggregates being formed in thickener feedwells. The G400 probe consistently measures larger chord lengths, and this is seen as a significant advantage. Of course, aggregates are rarely spherical, in some instances becoming quite elongated. It is, therefore, a consequence of the square-weighting applied to such chords that the mean values may in fact be much larger than for more spherical aggregates. Given that the main use of FBRM is in detecting changes, this is not necessarily a concern, but something that users need to be alert to.

Another consequence of measuring larger chord lengths, which inevitably contribute only a low number of counts, is a greater degree of noise in the square-weighted distributions, as evident in Figures 8 and 9. Such noise can be reduced by acquiring the chord length data over longer time intervals or averaging over multiple measurements. This is viable in continuous processes such as flocculation in a pipe reactor, but attempting this in a batch reactor or a full-scale feedwell risks the masking of true peaks in aggregate size or process fluctuations. In reality, the magnitudes of the changes that can be detected from swings in flocculation performance are sufficiently large that they should exceed any contributions from such noise. The results obtained in this study were acquired every 2 s and averaged over five consecutive measurements, but only after checking that this did not influence the trends; longer measurement durations would only be considered for much slower processes.

Although the chord length measurement principle applied with the G400 probe leads to an enhanced sensitivity to species at the lower end of the measurement range relative to previous generation FBRM, the lower limit still remains around 1 μm. For the vast majority of hydrometallurgical applications this is of little concern, particularly given the ionic nature of most process liquors and the likelihood of colloidal particles being aggregated. However, this limit remains well above what would be considered appropriate for the direct study of nanoparticles, and the detection of aggregation of such particles may only be practical in limited circumstances.

Summary

The main attraction of FBRM has always been real-time direct monitoring of particle systems without the need for dilution, highly desirable in most applications but absolutely essential in flocculation studies. The aggregates formed are fragile, and for the majority of mineral systems, irreversibly ruptured by excess shear. Assessing a flocculation process should involve estimating both the size of the aggregates formed and the efficiency of fines capture, information readily derived from FBRM through the square-weighted and unweighted chord length distributions, respectively. The measurement of chord lengths with the new generation G-series instruments by setting a much lower reflected intensity threshold substantially enhances the information obtained from flocculated systems by FBRM. The probability of measuring chord lengths more representative of larger aggregates is increased, while clearer discrimination of the contribution of fine particles or small aggregates to the unweighted chord length distributions greatly increases the value of FBRM in screening products or conditions that lead to inefficient aggregation.

Acknowledgments

The authors thank Nancy Hanna, Shaun O'Donnell, and Gay Walton for Malvern size measurements, and Alton Grabsch and Jon Halewood for experimental assistance. Ben Smith (Mettler-Toledo AutoChem) is thanked for useful discussions. Financial assistance and support from the Parker Centre for Integrated Hydrometallurgy Solutions, Curtin University, and CSIRO to A. Senaputra is also gratefully acknowledged.

Literature Cited

1. Gregory J. Fundamentals of flocculation. *Crit Rev Environ Control*. 1989;19:185–230.
2. Ayyala S, Pugh RJ, Forssberg E. Aggregate characteristics in coagulation and flocculation. *Miner Process Extract Metall Rev*. 1995;12:165–184.
3. Heath AR, Bahri PA, Fawell PD, Farrow JB. Polymer flocculation of calcite: relating the aggregate size to the settling rate. *AIChE J*. 2006;52:1987–1994.
4. Farrow JB, Warren LJ. The measurement of floc density-floc size distributions. In: Moudgil BM, Scheiner BJ, editors. Flocculation and Dewatering. New York: Engineering Foundation, 1989:153–166.
5. Gagnon MJ, Leclerc A, Simard G, Peloquin G. A fractal model for the aggregate size distribution generated by red mud flocculation. In: Crepeau, PN, editor. Light Metals. Warrendale, PA: TMS, 2003:105–111.
6. Heffels C, Polke R, Rädle M, Sachweh B, Schäfer M, Scholz N. Control of particulate processes by optical measurement techniques. *Part Part Syst Charact*. 1998;15:211–218.
7. Spicer PT, Pratsinis S, Raper J, Amal R, Bushell G, Meesters G. Effect of shear schedule on particle size, density, and structure during flocculation in stirred tanks. *Powder Technol*. 1998;97:26–34.
8. Gregory J, Nelson DW. Monitoring of aggregates in flowing suspensions. *Colloids Surf*. 1986;18:175–188.
9. Spears DR, Stanley DA. Study of shear-flocculation of silica. *Miner Metall Process*. 1994;11(1):5–11.
10. Murphy DD, Bakker MG, Spears DR. New insights into the mechanism of shear-flocculation of silica with fatty acids. *Miner Metallurgical Process*. 1994;11(1):26–30.
11. Caron-Charles M, Gozlan JP. Improvement of the floc resistance to a centrifugal shear field by polymer adjunction. *Chem Eng Sci*. 1996;51:4649–4659.
12. Sengupta DK, Kan J, Al Taweel AM, Hamza HA. Dependence of separation properties on flocculation dynamics of kaolinite suspension. *Int J Miner Process*. 1997;49:73–85.
13. Williams RA, Peng SJ, Naylor A. In situ measurement of particle aggregation and breakage kinetics in a concentrated suspension. *Powder Technol*. 1992;73:75–83.
14. Peng SJ, Williams RA. Control and optimization of mineral flocculation and transport processes using online particle-size analysis. *Miner Eng*. 1993;6:133–153.
15. Peng SJ, Williams RA. Direct measurement of floc breakage in flowing suspensions. *J Colloid Interface Sci*. 1994;166:321–332.
16. Fawell P, Richmond W, Jones L, Collisson M. Focused beam reflectance measurement in the study of mineral suspensions. *Chem Aust*. 1997;64(2):4–6.
17. Dippenaar A. *Shear Flocculation of Fines for Improved Flotation. Mintek Report No. M230*. Randburg: Council for Mineral Technology, 1985.
18. Blanco A, Fuente E, Negro C, Tijero J. Flocculation monitoring: focused beam reflectance measurement as a measurement tool. *Can J Chem Eng*. 2002;80:734–740.
19. Negro C, Blanco A, San Pio I, Tijero J. Methodology for flocculant selection in fibre-cement manufacture. *Cement Concrete Compos*. 2006;28:90–96.
20. Jarabo R, Fuente E, Moral A, Blanco A, Izquierdo L, Negro C. Effect of sepiolite on the flocculation of suspensions of fibre-reinforced cement. *Cement Concrete Res*. 2010;40:1524–1530.
21. Hecker R, Kirwan L, Jefferson A, Fawell PD, Farrow JB, Swift JD. Focussed beam reflectance measurement for the continuous

assessment of flocculant performance. *The Use of Polymers in Mineral Processing. 3rd UBC McGill Bi-Annual International Symposium on Fundamentals of Mineral Processing*. Montreal: Canadian Institute of Mining, Metallurgy and Petroleum, 1999:91–105.
22. Owen AT, Fawell PD, Swift JD. The preparation and ageing of acrylamide/acrylate copolymer flocculation solution. *Int J Miner Process*. 2007;84:3–14.
23. Swift JD, Simic K, Johnston RRM, Fawell, PD, Farrow, JB. A study of the polymer flocculation reaction in a linear pipe with a focused beam reflectance measurement probe. *Int J Miner Process*. 2004;73: 103–118.
24. Heath AR, Bahri PA, Fawell PD, Farrow JB. Polymer flocculation of calcite: experimental results from turbulent pipe flow. *AIChE J*. 2006;52:1284–1293.
25. Heath AR, Bahri PA, Fawell PD, Farrow JB. Polymer flocculation of calcite: population balance model. *AIChE J*. 2006;52:1641–1653.
26. Owen AT, Fawell PD, Swift JD, Labbett DM, Benn FA, Farrow JB. Using turbulent pipe flow to study the factors affecting polymer-bridging flocculation of mineral systems. *Int J Miner Process*. 2008; 87:90–99.
27. Fawell PD, Owen AT, Grabsch AF, Benn FA, Labbett DM, Swift JD. Factors affecting flocculation within gravity thickeners. *Water in Mining 2009: Proceedings*. Carlton, Australia: AusIMM, 2009:71–76.
28. Kirwan LJ. Investigating bauxite residue flocculation by hydroxamate and polyacrylate flocculants utilising the focussed beam reflectance measurement probe. *Int J Miner Process*. 2009;90:74–80.
29. Phillips EC. Continued efforts on the development of salicylic acid containing red mud flocculants. In: Tabereaux AT, editor. Light Metals. Warrendale, PA: TMS, 2004:21–26.
30. Thapa KB, Qi Y, Hoadley AFA. Interaction of polyelectrolyte with digested sewage sludge and lignite in sludge dewatering. *Colloids Surf A Physicochem Eng Asp*. 2009;334:66–73.
31. De Clercq B, Lant PA, Vanrolleghem PA. Focused beam reflectance technique for in situ particle sizing in wastewater treatment settling tanks. *J Chem Technol Biotechnol*. 2004;79:610–618.
32. Greaves D, Boxall J, Mulligan J, Montesi A, Creek J, Sloan ED, Koh CA. Measuring the particle size of a known distribution using the focused beam reflectance measurement technique. *Chem Eng Sci*. 2008;62:5410–5419.
33. Vay K, Frieß W, Scheler S. Understanding reflection behavior as a key for interpreting complex signals in FBRM monitoring of microparticle preparation processes. *Int J Pharm*. 2012;437;1–10.
34. Heath AR, Fawell PD, Bahri PA, Swift JD. Estimating average particle size by focused beam reflectance measurement (FBRM). *Part Part Syst Charact*. 2002;19:84–95.
35. Smith B. *The Next Generation FBRM® (Focused Beam Reflectance Measurement)*. Mettler-Toledo AutoChem. Available at: http://tinyurl.com/d9ounu6, accessed on March 19, 2013.
36. Hogg R. The role of polymer adsorption kinetics in flocculation. *Colloids Surf A Physicochem Eng Asp*. 1999;146:253–263.
37. Malito JT. Improving the operation of red mud pressure filters. In: Hale W, editor. Light Metals. Warrendale, PA: TMS, 1996:81–85.
38. Xu B, Smith P, Wingate C, De Silva L. The effect of calcium and temperature to the transformation of sodalite to cancrinite in Bayer digestion. *Hydrometallurgy*. 2010;105:75–81.
39. Evans K, Nordheim E, Tsesmelis K. Bauxite residue management. In: Suarez CE, editor. Light Metals. Warrendale, PA: TMS, 2012: 63–66.
40. Jones F. The mechanism of Bayer residue flocculation. PhD Thesis. Perth: Curtin University, 1998.
41. Hulston J. Effect of flocculation conditions on the dewaterability of hematite and red mud suspensions. PhD Thesis. Melbourne: The University of Melbourne, 2005.
42. Hukkanen EJ, Braatz RD. Measurement of particle size distribution in suspension polymerization using in situ laser backscattering. *Sensor Actuat B*. 2003;96:451–459.
43. ISO 13320:2009(E): Particle Size Analysis – Laser Diffraction Methods. Geneva: ISO, 2009.
44. Alfano JC, Carter PW, Gerli A. Characterization of the flocculation dynamics in a papermaking system by non-imaging reflectance scanning laser microscopy (SLM). *Nordic Pulp Paper Res J*. 1998;13(2): 159–165.
45. Grabsch AF, Fawell PD, Adkins SJ, Beveridge A. The impact of achieving a higher aggregate density on polymer-bridging flocculation. *Int J Miner Process*. 2013;124:83–94.

Manuscript received Mar. 29, 2013, and revision received Aug. 20, 2013.